

Estimating Fixed Frame Galaxy Magnitudes in the SDSS¹

Michael R. Blanton², J. Brinkmann⁷, István Csabai³, Mamoru Doi⁴, Daniel Eisenstein⁵, Masataka Fukugita^{8;9}, James E. Gunn⁶, David W. Hogg², and David J. Schlegel⁶

ABSTRACT

Broad-band measurements of flux for galaxies at different redshifts measure different regions of the rest-frame galaxy spectrum. Certain astronomical questions, such as the evolution of the luminosity function of galaxies, require transforming these inherently redshift-dependent magnitudes into redshift-independent quantities. To prepare to address these astronomical questions, investigated in detail in subsequent papers, we fit spectral energy distributions (SEDs) to broad band photometric observations, in the context of the optical observations of the Sloan Digital Sky Survey (SDSS). Linear combinations of four spectral templates can reproduce the five SDSS magnitudes of all galaxies to the precision of the photometry. Expressed in the appropriate coordinate system, the locus of the coefficients multiplying the templates is planar, and in fact nearly linear. The resulting reconstructed SEDs can be used to recover fixed frame magnitudes over a range of redshifts. This process yields consistent results, in the sense that within each sample the intrinsic colors of similar type galaxies are nearly constant with redshift. We compare our results to simpler interpolation methods and galaxy spectrophotometry from the SDSS. The software that generates these results is publicly available and easily adapted to handle a wide range of galaxy observations.

Subject headings: galaxies: fundamental parameters | galaxies: photometry | galaxies: statistics

1. Motivation

In the future, observations of galaxies (and indeed of any astronomical sources) will be performed using devices which combine high spatial resolution and high spectral resolution. By that time, the phenomena of broad band filters and the quaint terminology surrounding their usage — magnitudes, K -corrections, color terms, etc. — will have long since been forgotten. However, today, virtually all observations of galaxies are

¹Based on observations obtained with the Sloan Digital Sky Survey

²New York University, Department of Physics, 4 Washington Place, New York, NY 10003

³Department of Physics and Astronomy, The Johns Hopkins University, Baltimore, MD 21218

⁴Department of Astronomy and Research Center for the Early Universe, School of Science, University of Tokyo, Tokyo 113-0033, Japan

⁵Steward Observatory, 933 N. Cherry Ave., Tucson, AZ 85721

⁶Princeton University Observatory, Princeton, NJ 08544

⁷Apache Point Observatory, 2001 Apache Point Road, P.O. Box 59, Sunspot, NM 88349-0059

⁸Institute for Cosmic Ray Research, University of Tokyo, Midori, Tanashi, Tokyo 188-8502, Japan

⁹Institute for Advanced Study, Olden Lane, Princeton, NJ 08540

made through such filters, and special care has to be taken to recover knowledge of galaxy spectral energy distributions (SEDs) from these observations. Reconstructing galaxy SEDs is nontrivial because SEDs of galaxies contain important information on scales considerably smaller than the width of typical broad band filters. Furthermore, SEDs of distant galaxies are redshifted such that the more distant the galaxy, the further the observed bandpass is blueshifted relative to the rest-frame spectral energy distribution of the object observed. This paper focuses on a solution to these problems which (in the optical wavelength regime) is fast, robust, and consistent over a large range of redshifts.

In the past, people have accounted for these effects using "K-corrections" applied to the observed magnitudes. In these analyses, a function $K(z)$ is added to the standard cosmological bolometric distance modulus $DM(z)$ to obtain the relationship between the apparent magnitude m and the absolute magnitude M :

$$m = M + DM(z) + K(z) \quad (1)$$

Sometimes a single function has been applied regardless of the galaxy type, though more recently it has become standard to use a discrete set of $K(z)$ functions depending on galaxy type (based either on morphology or spectral features). As described in Oke & Sandage (1968) and later papers, the function is based on the projection of an assumed galaxy SED redshifted to z onto the measured instrument response as a function of wavelength (including the effects of the atmosphere, the reflectivity of the mirrors, the filter transmission, and the response of the CCD device or photographic emulsion). For example, for the Sloan Digital Sky Survey (SDSS) filter system, Frei & Gunn (1994) and Fukugita, Shimazaki, & Ichikawa (1995) have both presented results for the K-corrections of galaxies. Each of these papers tabulates $K(z)$ (called $k(z)$ by Frei & Gunn 1994) for galaxies of various morphological types, based on galaxy spectrophotometry.¹⁰

However, galaxies do not all have the same SED, nor are they selected from some discrete set of SEDs. For this reason, these schemes for applying the K-corrections can fail to be self-consistent: the SED assumed for the K-corrections can be significantly inconsistent with the observed galaxy colors! As we demonstrate more precisely from our astronomical data analysis in new, large multi-band surveys, and in particular as we try to quantify the evolution of galaxies, we must take a more sophisticated approach to approximating redshifted observations of galaxies.

Our approach here is to use a method for inferring the underlying SEDs of a set of galaxies at a range of redshifts by requiring that their SEDs all be drawn from a similar population. For each galaxy, we will recover a model SED, which can be used to synthesize the galaxy's magnitude in any bandpass. Although the operation we are performing on the magnitudes is not a "K-correction" in the historical sense of the term, we will refer to it as such in this and subsequent papers. Our approach is equivalent (nearly identical) to the photometric redshift estimation methods of Casali et al. (2000), except we use slightly different coordinate systems for our SED template space. In fact, the software includes a fast and relatively accurate photometric redshift estimator based on their method.

We implemented this system and are publishing it in order to lay the groundwork for upcoming papers which will rely heavily on the reliability of the redshifted magnitudes determined here. Because the SDSS is one of the largest astronomical surveys to date, our method will be useful to a large number of other investigators, both inside and outside the SDSS collaboration. Thus, this paper also serves the purpose of describing the release of a piece of software. The computer software we distribute builds itself into a shared object library, around which we have written both stand-alone C programs and IDL routines. We have made

¹⁰Note that the description on p. 57 of Binney & Merrifield (1998) of the meaning of $k(z)$ in Frei & Gunn (1994) is incorrect; in fact, their $k(z)$ is exactly equivalent to our $K(z)$.

the source code available publicly, through a web page and through a public CVS repository. Improvements or ports to other languages implemented by users may be incorporated into the code upon request. The conditions of use for the code are that this paper is cited in any resulting refereed journal article and that the version of the code used is specified in any such paper. The version of the code used to make the figures for this paper is kcorrect v1.10.

We refer throughout this paper to AB magnitudes, first defined by Oke & Gunn (1983) such that:

$$\begin{aligned}
 m_{AB} &= 2.41 - 2.5 \log_{10} \frac{\int_{R_1}^{\infty} d^{-1} f(\lambda) R(\lambda) d\lambda}{\int_{R_1^0}^{\infty} d^{-1} f(\lambda) R(\lambda) d\lambda} ; \\
 &= 48.60 - 2.5 \log_{10} \frac{\int_{R_1}^{\infty} d^{-1} f(\lambda) R(\lambda) d\lambda}{\int_{R_1^0}^{\infty} d^{-1} f(\lambda) R(\lambda) d\lambda} ;
 \end{aligned}
 \tag{2}$$

where $R(\lambda)$ is the fraction of photons entering the Earth's atmosphere which are detected as a function of wavelength (a unitless quantity). In this equation, $f(\lambda)$ is in units of $\text{ergs cm}^{-2} \text{s}^{-1} \text{\AA}^{-1}$, and $f(\nu)$ is in units of $\text{ergs cm}^{-2} \text{s}^{-1} \text{Hz}^{-1}$. The normalizations defined here mean that an object with $f(\lambda) = 3631 \text{ Jy} = 3.631 \times 10^{20} \text{ ergs cm}^{-2} \text{s}^{-1} \text{Hz}^{-1}$ has all its AB magnitudes equal to zero. The difference in the zeropoint in the two equations simply corresponds to the factor of the speed of light c (expressed in \AA s^{-1}) between the frequency and wavelength scales.

Section 2 describes our method of fitting galaxy SEDs to broad band photometry and how to calculate K-corrections. Section 3 applies the method to galaxies in the SDSS, showing that the fits are robust. Section 4 concludes and discusses future development of the method described here.

2. Calculating Fixed Frame Galaxy Magnitudes

First, we describe how we reconstruct galaxy SEDs from broad band magnitude measurements. Second, we describe how we convert these SEDs into estimates of fixed frame galaxy magnitudes.

2.1. Fitting SEDs to Galaxy Broad-band Magnitudes

Our task is to recover a model for the galaxy SED from broad band photometric measurements. Since a set of broad band galaxy fluxes does not correspond uniquely to a particular SED, and because galaxy SEDs are known to have significant structure over wavelength ranges small compared to our bandpass, the inverse problem of reconstructing SEDs from broad band fluxes is ill-posed. The task is made yet more difficult by the fact that the separations of the filters are large compared to their widths; the SEDs are thus not well-sampled in the Nyquist sense of that term. However, we are not completely ignorant about the forms which galaxy SEDs take, so we can attempt to use what we know about galaxy SEDs to appropriately regularize our fits. The method described here for doing so follows closely the method of estimating photometric redshifts used by Casabian et al. (2000). It is designed to take advantage of what we already understand about galaxy spectral energy distributions.

Begin with an SED space defined by N_b template galaxy SEDs $v_i(\lambda)$ (for example from Bruzual & Charlot 1993), where N_b is large. In principle, this should be a complete set of galaxy SEDs if we want all galaxy SEDs to be in the space spanned by the $v_i(\lambda)$; in practice, this property is not necessary. Given a set of $v_i(\lambda)$, one can find an orthonormal set of spectra $b_i(\lambda)$ spanning the same space. To be more precise,

we define the dot-product in the space of galaxy spectra to be:

$$v_i \cdot v_j = \int_{\lambda_{min}}^{\lambda_{max}} v_i(\lambda) v_j(\lambda) d\lambda; \quad (3)$$

where λ_{min} and λ_{max} define the wavelength range used to define orthogonality. These limits are defined not over the full range covered by the $v_i(\lambda)$ spectra, but instead over a smaller range which is within observable wavelengths over most of the redshift range of the sample.¹¹ We then define the basis of the SED space such that the N_b template SEDs, v_i , are linear combinations of N_b basis spectra b_i and that $b_i \cdot b_j = \delta_{ij}$. These conditions do not fully specify the b_i , which naturally may be rotated arbitrarily within our N_b -dimensional subspace of spectral space.

In our case the number of observed bands is less than N_b , so we cannot determine an individual galaxy's position in this N_b -dimensional space from its broad band colors alone. However, as outlined by Csabai et al. (2000), one can find a lower dimensional space defined by N_c vectors e_k which best fits the set of galaxies, as follows. The SED of galaxy i may be reconstructed from a linear combination of the basis spectra in this lower dimensional space:

$$f_{rec;i}(\lambda) = \sum_k a_{i;k} \sum_j e_{k;j} b_j(\lambda); \quad (4)$$

where a_k are the components of the galaxy projected in the low-dimensional space. From this SED it is easy to determine the reconstructed flux $F_{rec;i;l}$ in each survey bandpass by projecting the model SED onto the bandpass l :

$$F_{rec;i;l} = \int_0^1 f_{rec;i}(\lambda) S_l(\lambda) d\lambda; \quad (5)$$

where $S_l(\lambda)$ is the response of the instrument in band l . We define

$$\chi^2 = \sum_i \sum_l \frac{(F_{obs;i;l} - F_{rec;i;l})^2}{\sigma_{il}^2}; \quad (6)$$

where σ_{il} is the estimated error in the observed flux $F_{obs;i;l}$ in bandpass l for galaxy i . Taking derivatives of χ^2 with respect to $a_{i;k}$ and $e_{k;j}$ results in a set of equations bilinear in $a_{i;k}$ and $e_{k;j}$. Csabai et al. (2000) describe how to iteratively solve this bilinear equation by first fixing $e_{k;j}$ and fitting for $a_{i;k}$, then fixing $a_{i;k}$ and fitting for $e_{k;j}$, and iterating that procedure.

We define the "total flux" of each template as the flux in the range $\lambda_{min} < \lambda < \lambda_{max}$; then an estimate of the flux in this range is $F_t = \sum_k a_k f_k$. Galaxies of some fixed F_t clearly lie on a plane in the component space a_k . Therefore, a natural choice for the orientation of the axes e_k is to let e_0 be perpendicular to the planes of constant F_t ; in this manner, the coefficient a_0 in Equation (4) is directly proportional to F_t and is thus purely a measure of the object's flux (in the wavelength range $\lambda_{min} < \lambda < \lambda_{max}$), while the parameters $a_i = a_0$ (where $i > 0$) primarily measure the shape of the galaxy SED in the wavelength range $\lambda_{min} < \lambda < \lambda_{max}$. F_t can be trivially related to L_t , the total luminosity in this range, by the inverse square of the luminosity distance (from, for example, Hogg 1999). As it turns out, the parameters $a_i = a_0$ tend to be distributed approximately in an ellipsoid, with not much curvature within the space defined by the template SEDs. Thus, we transform the axes such that $a_i = a_0 = 0$ is the mean of the distribution and rotate the axes e_i (for $i > 0$) such that they are aligned with the principal axes of the ellipsoid. Furthermore, we normalize

¹¹If the template spectra were identical in the subrange chosen and only differed outside of it, our choice would cause computational problems, but in fact the spectra are all independent in the restricted, as well as the full, wavelength range.

the vectors e_i such that the zeroth component $a_0 = F_t$ is output by the code in units of $\text{ergs cm}^{-2} \text{s}^{-1}$ (within the range $m_{\text{in}} < < m_{\text{ax}}$).

In this way, we can reconstruct SEDs based on the broad band magnitudes of galaxies. From these reconstructed SEDs one can estimate K-corrections, develop a measure of galaxy spectral type, or synthesize other measurements of galaxy flux. The templates determined during the procedure can, of course, be used to estimate photometric redshifts, as Casajet al. (2000) describes.

2.2. Applying Direct Constraints on $a_i=a_0$

Sometimes we will want to apply direct constraints on the coefficients $a_i=a_0$ of the galaxy we are fitting. For example, in this paper we fit our templates to a set of galaxies with high quality photometry in all bands. However, we would like to use these templates to fit for the SEDs of other galaxies, which might have much worse photometry in one or more bands. Since the errors in the photometry can be catastrophic (that is, non-gaussian), when we fit the SEDs of the lower signal-to-noise galaxies it makes sense to at least weakly constrain these galaxies to have reasonable SEDs, in the sense that the $a_i=a_0$ ought not to be too different than those for well-measured galaxies. We can assume a gaussian prior probability distribution with a mean $\hat{a}_{c;j}=a_{c;0}i$, a variance matrix $V_{c;j;l}$, and a weight A_c . We calculate a preliminary value of $\hat{a}_{c;0}$, assuming $a_i = 0$. Then we constrain our fit by adding a term to χ^2 as follows:

$$\chi^2 = \chi^2 + \sum_j A_c V_{j;l}^{-1} \left(\frac{a_1}{\hat{a}_{c;0}} - \frac{a_{c;l}}{a_{c;0}} - \frac{a_j}{\hat{a}_{c;0}} - \frac{a_{c;j}}{a_{c;0}} \right)^2 \quad (7)$$

The resulting χ^2 can still be minimized linearly, so we have sacrificed very little in speed. Note that with such a constraint, one can calculate K-corrections even for galaxies with only one or two bands measured, and still obtain sensible results.

2.3. Calculating K-corrections

We here define a notation which we will use in subsequent papers for the effective rest-frame bandpass at any redshift in band b, namely:

$$\bar{z}_b \quad (8)$$

read, "b-band at redshift z." For example, if we measure the flux of a galaxy at $z = 0.22$ using a g-band filter, we have obtained the $^{0.22}g$ -band magnitude of the galaxy. The goal of "K-correction" is to convert the ugriz bands at redshift z for each galaxy to ugriz bands at some fixed redshift \bar{z}_0 .

Given AB galaxy magnitudes m and errors for a galaxy at redshift z, one can use the method of the previous subsection to reconstruct the galaxy rest-frame SED. With this reconstruction in hand, it is straightforward to project the SED onto any bands at any redshift z_0 (cf. Equation 2):

$$\begin{aligned} z_0 m_{\text{rec}} &= 2.41 - 2.5 \log_{10} \frac{\int_0^{R_1} d \frac{f_{\text{rec}}}{R^{1+z_0}} (\frac{1}{1+z_0}) R () \#}{\int_0^{R_1} d^{-1} R ()} \\ &= 48.60 - 2.5 \log_{10} \frac{\int_0^{R_1} d^{-1} (1+z_0) f_{\text{rec}} [(1+z_0) R () \#}{\int_0^{R_1} d^{-1} R ()} \end{aligned} \quad (9)$$

The simple way to remember where the factors of $(1+z)$ appear in these equations is to remember that K -corrections are defined to be the change in magnitude with redshift for fixed bolometric flux. So when the spectrum is stretched by the $(1+z_0)$ redshift factor, as in $f(\lambda) = f(\lambda/(1+z_0))$, the bolometric flux should be constant; that is, you must apply the extra multiplicative factor $1/(1+z_0)$ to counteract the stretching of the spectrum.

Given the reconstructed magnitudes, one can calculate the fixed frame magnitudes in one of two ways:

1. Simply use $z_0 m_{rec}$, the reconstructed magnitudes at redshift z_0 , as the fixed frame magnitudes.
2. Use the difference $z_0 m_{rec} - z m_{rec}$ as an estimate of the correction to apply to the observed $z m$.

If the reconstructions $z m_{rec}$ are very similar to the actual observations $z m$ (as we will show is the case for our fits), there is very little difference between these two methods. However, if the reconstructions are poor, there will be large differences between the methods; in particular, method (1) will yield a color distribution of galaxies with artificially low dimensionality. Having estimated $z_0 m$, you can then calculate the luminosity by simply applying to the calculated magnitude the cosmological distance modulus (that is, the luminosity distance-squared law, as tabulated by, e.g., Hogg 1999).

We want to emphasize here that, while K -correcting to a fixed frame bandpass is sometimes necessary in order to achieve a scientific objective, it is not always necessary or appropriate. Because K -corrections are inherently uncertain (the broad band magnitudes do not uniquely determine the SED) they should be avoided or minimized when possible. For example, if one were calculating the evolution of clustering of red and blue galaxies separately, it would perhaps be wise to perform the separation not on the K -corrected colors of the galaxies but on the median color of M galaxies as a function of redshift. Similarly, in situations where K -corrections cannot be ignored, such as the calculation of the evolution of the luminosity function, their effect should be minimized by, for example, correcting to the median redshift of galaxies in the sample.

Typically one's measurements will be difficult to connect to solar luminosities in z_b (unless $z = 0$), simply because nobody has projected the appropriate stellar spectrophotometry onto these bandpasses. However, it is our position that stars are better understood than galaxies, and that it is therefore simpler in the end to stay as close as possible to the system in which the galaxies are observed. In any case, astronomy is quickly reaching a level of precision for which the exact nature of the bandpasses used has to be known and considered in most analyses of observational data.

The reader may ask why, if we are basing our K -corrections on a full model of the galaxy SED, we do not correct to bandpasses with simpler shapes (for example, top hats). The reason is that we want the effective bandpasses to actually have been observed for some galaxies in the sample, so that the K -correction for those galaxies are formally and actually zero. This property is desirable because, as noted above, there are inherent uncertainties in the K -corrections. Nevertheless, we note that synthesizing top hat magnitudes may be appropriate in certain situations, as they have the virtue (similarly to the AB magnitude system) that they are very easy to comprehend and synthesize from theory.

2.4. Public Access to the Code

The version of the K -correction code (v1.10) implementing the calculations described here, along with eigentemplates and filter curves, is publicly available on the World Wide Web at <http://physics.nyu.edu/~mb144/kcorrect>. The whole of the code can be used through the Research Systems, Incorporated, IDL

language; everything except for the templating also exists in stand-alone C programs (which call the same routines, guaranteeing consistency).

3. Application to SDSS Data

In this section we describe how we applied the above method to the SDSS data set.

3.1. SDSS Spectroscopic Data

The SDSS (York et al. 2000) is producing imaging and spectroscopic surveys over $\sim 10^4$ steradians in the Northern Galactic Cap. A dedicated 2.5m telescope (Siegmond et al., in preparation) at Apache Point Observatory, Sunspot, New Mexico, images the sky in five bands between 3000 and 10000Å (u, g, r, i, z; Fukugita et al. 1996) using a drift-scanning, mosaic CCD camera (Gunn et al. 1998), detecting objects to a flux limit of $r^0 \sim 22.5$. The ultimate goal is to spectroscopically observe 900,000 galaxies, (down to $r_{\text{lim}}^0 \sim 17.65$), 100,000 Luminous Red Galaxies (LRGs; Eisenstein et al. 2001), and 100,000 QSOs (Fan 1999; Newberg et al., in preparation). This spectroscopic follow up uses two digital spectrographs on the same telescope as the imaging camera. Many of the details of the galaxy survey are described in a description of the galaxy target selection paper (Strauss et al. 2002). Other aspects of the survey are described in the Early Data Release (EDR; Stoughton et al. 2002).

The results of the photometric pipeline for all of the galaxies were extracted from the SDSS Operational Database. The photometry used here for the bulk of these objects was the same as that used when the objects were targeted. However, for those objects which were in the EDR photometric catalog, we used the better calibrations and photometry from the EDR. The versions of the SDSS pipeline PHOTO used for the reductions of these data ranged from v5_0 to v5_2. The treatment of relatively small galaxies, which account for most of our sample, did not change substantially throughout these versions. As described in Smith et al. (2002), magnitudes are calibrated to a standard star network approximately in the AB system, described in Section 1.

The response functions $R(\lambda)$ of the filter-CCD combinations have been measured using a monochromator by Mamoru Doi. Using a model for the atmospheric transmission and the reflectivity of the primary and secondary mirrors, one can then model the response of the entire system. For each bandpass in the SDSS, there are six different CCDs; it has been shown that the differences between these six camera columns are small; what differences exist are largely λ out during the survey calibration. The resulting set of filter curves is shown in Figure 1, in comparison to a model of a galaxy spectral energy distribution observed at $z = 0$ (a 4 Gyr old instantaneous burst from the models of Bruzual & Charlot 1993).

The results of the spectroscopic observations are treated as follows. We extract one-dimensional spectra from the two-dimensional images using a pipeline (specBS v4_8) created specifically for the SDSS instrumentation (Schlegel et al. 2002), which also λ ts for the redshift of each spectrum. The official SDSS redshifts are obtained from a different pipeline (SubbaRao et al. 2002). The two independent versions provide a consistency check on the redshift determination. They are consistent (for galaxies) at over the 99% level.¹²

¹²The official pipeline currently tends to work better for objects with unusual spectra, such as certain types of stars and QSOs.

We use two types of magnitudes determined by the SDSS. First, the SDSS Petrosian magnitudes, a modified form of the magnitude described by Petrosian (1976), as described in Strauss et al. (2002). These magnitudes have a nearly constant metric aperture as a function of redshift; in addition, all the bands use the same aperture, so the measured SED corresponds (to within the effects of seeing) to the SED of an identifiable region of the galaxy. However, for faint objects, the Petrosian magnitudes tend to become noisy. Thus, for galaxies with $z > 0.25$ we instead use the higher signal-to-noise model magnitudes. Model magnitudes are calculated in all bands using a single weighted aperture; thus, the measured colors again correspond to an identifiable region of the galaxy, though a different one than would be measured by the Petrosian magnitude. The weighted aperture is the better fitting model (pure exponential or pure de Vaucouleurs) to the galaxy image in the r-band. In Stoughton et al. (2002) we are explicitly warned not to mix Petrosian and model magnitudes in a single analysis, since they measure galaxies in very different ways. Nevertheless, for the purposes of constraining galaxy template SEDs, it is perfectly acceptable to use any well-defined part of any galaxy. For our purposes, it is more important to have high signal-to-noise measurements of galaxy colors than to measure exactly the same regions of galaxies at low and high redshift. We extinction-correct both types of magnitudes using the dust maps of Schlegel, Finkbeiner & Davis (1998).

3.2. Fitting SEDs to SDSS Data

For the purposes of applying the method described in Section 2 to SDSS data, we take a subsample of the data consisting of around 30,000 objects in the range $0.0 < z < 0.5$. The sample includes both the main sample and the LRGs; we sample these spectra such that we get an approximately even distribution within our range of redshifts. In addition, we add results from galaxies in several plates (totalling about 1,000 objects) which were selected by a photometric redshift algorithm (Casabian et al., in preparation) to be at around $z = 0.3 \pm 0.4$. These objects are invaluable for tying down the blue end of the templates. Finally, we exclude galaxies in the redshift range $0.28 < z < 0.32$ from the fit for the templates, for reasons which we will explain more fully below (nevertheless, we still can and do use the resulting templates to analyze galaxies in this range).

Some of the objects have missing or poorly constrained data. For example, the u- or z-band fluxes for some objects are swamped by the photon noise of the sky. We identify such cases as magnitude errors greater than 2.0 or magnitudes fainter than 24.0 in any band. We ignore these objects entirely when fitting for the templates. However, we still want to determine a best-fit SED for each object, once the templates are determined. Thus, after the templates have been determined, we constrain all the SED fits to all galaxies using the method described in Section 2.2. As a constraint, we use the covariance matrix and mean value (essentially zero, by design) of the coefficients of the well-measured set of galaxies used to determine the templates; we multiply all the elements of the covariance matrix by a factor of four to weaken our constraint (which is appropriate, since the actual distribution of coefficients is not well described by a single gaussian). Thus, we account for the missing information by simply requiring that the object SED have "reasonable" properties. The constraint does not affect the results for galaxies which have well-measured magnitudes in all bands.

In addition, the photometric errors for most objects in the spectroscopic galaxy sample of the SDSS are not dominated by the estimated errors on the photometry listed in the catalog. Instead, the errors are dominated by local calibration errors and other systematic effects, which are poorly known. To account for these errors, we add extra error terms in quadrature with the errors listed in the catalog (0.05 mags, 0.02 mags, 0.02 mags, 0.02 mags, and 0.03 mags for ugriz, respectively). Not accounting for this extra source of

errors can cause the fits to be ill-behaved.

For the SED space (our $v_i(\lambda)$), we use the subspace defined by linear combinations of ten Bruzual-Charlot instantaneous burst models with ages ranging from 3×10^7 to 2×10^{10} years, we with metallicity $Z = 0.02$ and we with $Z = 0.004$, all assuming a Salpeter Initial Mass Function. Since we cannot recover information about the SED below a certain wavelength scale, we smooth most of the wavelength regime of the templates using a Gaussian with a standard deviation of $\sigma = 300\text{\AA}$; for the region of the spectrum which contains the sharpest gradients, around 4000\AA , we smooth only with $\sigma = 150\text{\AA}$. None of our results change dramatically if we vary our smoothing procedure or if we add reddened templates to our allowed SED space.

We choose to fit for $N_t = 4$ eigen templates, the maximum one can use and still allow freedom to fit for the templates themselves. Simply using five templates (which obviously reproduces all the magnitudes exactly) tends to yield unphysical trends of galaxy SED versus redshift (cf. Figure 6 below). Using three templates does nearly as well as four templates in the sense that the resulting templates reproduce the griz magnitudes nearly as well. However, the fourth template is necessary to recover the u-band flux to any better than about 15%. In addition, since one of the applications of these SED determinations is the distribution of galaxy colors in fixed frame magnitudes, we don't want to artificially reduce the dimensionality of the color space to only two.

One more choice needs to be made, the wavelength regime over which to orthogonalize the templates and over which to calculate the flux. We choose the range defined by $\lambda_{\min} = 3500\text{\AA}$ and $\lambda_{\max} = 7500\text{\AA}$, since this range is included for almost all galaxies in the sample. We refer here and in other papers to the flux and luminosity in this range as the "visual flux" f_v and the "visual luminosity" L_v .

3.3. The g/r Gap

In Figure 1, there is clearly a gap between the g and r bands. Linear fits to the data allow considerable freedom in the resulting reconstructed SEDs. As it happens, one of the directions in our best fit coefficient space $a_1 = a_0$ corresponds to a large spike at around 4000\AA ; that this direction is important is not surprising, since one of the most variable quantities of galaxy SEDs is the size of the 4000\AA break. However, the gap between the g and r bands corresponds to the 4000\AA break at around $z = 0.3$. The existence of this spike in one direction in our four-dimensional space means that galaxies at $z = 0.3$ can vary along this direction in order to better fit u, i, and z, with little effect on the g-r color of the fit. This results in unphysical SED fits to galaxies near $z = 0.3$.

To demonstrate this degeneracy, Figure 2 shows the spectrum corresponding to the direction represented by the vector $e_2 + 0.7e_3$, for our best fit templates. We overplot the $^{0.3}g$ and $^{0.3}r$ bands. This direction has a strong peak in the gap between the two bands at $z = 0.3$. This difficulty is why, in Section 3, we exclude the regime around $z = 0.3$; otherwise the templates became distracted by the degeneracies in this range.

We have explored using a larger set of input spectrum, by including reddened versions of all our templates, to test whether a more complete space of SEDs would cause our fit to choose a more realistic subspace. In addition, we have tried removing the increased resolution of the template SEDs around the 4000\AA break. Neither of these tests yielded better results.

Our view is that the ideal solution to this problem would be to minimize χ^2 under the constraint that none of the original Bruzual-Charlot spectra defining our SED space contribute negatively to the SED fit. Such a solution would almost certainly have better properties than our linear approach here: it would almost

certainly avoid the degeneracies, it would yield reasonable SED over a larger wavelength range, it would associate a reasonable star-formation history with each object (which could be used to evolution-correct the magnitudes).

However, we have not tackled this approach yet. As it happens, the direct constraint on the coefficients described in the previous section is sufficient to suppress the g/r gap problem for many purposes, as long as one K-corrected the magnitudes to $z = 0.3$. In this way, one minimizes the K-corrections for the galaxies which one is least certain of.

One really only needs to worry about this effect in the SDSS when you are dealing with the LRGs, for galaxies in the range about $0.27 < z < 0.33$. The Main Sample results are not significantly affected at all. Furthermore, one can still observe a galaxy at $z = 0.1$ and reliably infer what it would look like at $z = 0.3$; it is only the reverse process which is difficult.

3.4. Results

The top two panels of Figure 3 show the pairwise joint distributions of $a_1=a_0$, $a_2=a_0$, and $a_3=a_0$ for a random subset of about 10,000 of the galaxies in the SDSS sample (not only the ones which we used to fit the templates). In the bottom panel, three spectra taken from a one-dimensional sequence along the galaxy locus are shown, showing that the spectra become progressively bluer along that sequence. Note that constraints on the SED become poor at the bluest and reddest edges of this diagram (the peak of the z-band response is at 8700 Å restframe for a galaxy observed at $z = 0$). Therefore, the odd behavior near the edges should not be taken too seriously. In addition, note the small spur extending from lower left to upper right through the right edge of the $(a_3=a_0)$ - $(a_2=a_0)$ plane. Many of the objects in this spur are at around $z = 0.3$, and this spur is the result of the degeneracy due to the g/r gap.

These reconstructed spectra do an excellent job of reproducing the observed galaxy fluxes. Figure 4 shows the differences between the observed and reconstructed fluxes as a function of redshift. There are no systematic trends with redshift, and the standard deviations of the differences between the observed and the reconstructed fluxes (shown on the right bottom corner of each panel) are of order the photometric errors in the sample. In particular, for our 30,000 galaxies (and thus approximately 30,000 degrees of freedom) we find $\chi^2 = 55,000$, indicating that our fit is reasonable.

An important test of the consistency of the fits is to check that for a fixed type of galaxy, the distribution of the fixed frame colors depends only weakly on redshift. Because the galaxies shown in Figures 3 and 4 are inhomogeneously selected — some are Main Sample galaxies, some are LRGs, and some are selected from the photometric redshift plates — we will split our sample into two well-defined sets of objects to perform this test. First, we choose a set of Main Sample galaxies in the luminosity range $-21.5 < M_{0.1r} < -21.2$. Figure 5 shows the observed-frame colors of all the galaxies as a function of redshift. The right-hand panels show the distribution for redshifts $0.05 < z < 0.10$ (solid histogram) and $0.10 < z < 0.17$ (dotted histogram). A trend exists in all colors, most strongly in $z(g-r)$. Figure 6 shows the K-corrected colors $^{0.1}(u-g)$, $^{0.1}(g-r)$, $^{0.1}(r-i)$, and $^{0.1}(i-z)$ in the same manner. The plots show a general consistency in the fixed frame color distribution of these objects with redshift. Small changes are discernible in the distributions, mostly attributable to the increased errors at higher redshift. Note that for $z < 0.1$ the $^{0.1}(u-g)$ color depends on an extrapolation of the SED in the blue, while for $z > 0.1$ the $^{0.1}(i-z)$ color depends on an extrapolation of the SED in the red.

Second, we choose a set of Cut I LRGs (see Eisenstein et al. 2001 for details) with $22.8 < M_{0.3z} < 22.5$. Figure 7 shows the observed colors as a function of redshift for these objects. Again, there is a strong redshift dependence. Figure 8 shows the colors K -corrected to $z = 0.3$, which appear approximately constant with redshift. $^{0.3}(g-r)$ (which is very similar to $^{0.0}(u-g)$) experiences a blueward shift of about 0.1 magnitudes between $z = 0.1$ and $z = 0.45$, which is attributable to passive evolution.

In short, these fits to galaxy SEDs provide estimates which reproduce the galaxy photometry nearly to the level of the errors in the photometry itself, seem physically reasonable, and are consistent over the range of redshifts we consider ($0.0 < z < 0.5$).

3.5. K -corrections in the SDSS

We show, in Figure 9, the resulting K -corrections to $z = 0.3$ inferred from this method, for all five SDSS bands. Note that the K -corrections are largest (and thus most uncertain) in $^{0.3}u$ and $^{0.3}g$. Remember that the K -corrections to $^{0.3}u$ are extrapolations for $z < 0.3$ and that the K -corrections to $^{0.3}z$ are extrapolations for $z > 0.3$, so those results should not be taken too seriously. (Although the K -corrections given are not too unreasonable).

An important test of our method is to synthesize broad band photometry from spectra, and then try to recover the K -corrections in a case where we know the spectrum completely. For this purpose, we use as example spectra the spectra of galaxies in the SDSS. Since we cannot synthesize the observed u and z bands, we simply base them on the synthesized g and i band magnitudes plus the $u-g$ and $z-i$ colors. (This procedure is unlikely to make the photometric estimates of the K -corrections better). Finally, we added 2% random errors to all of the measurements. Figure 10 compares the K -corrections from the synthesized photometry to that calculated from the spectrum itself:

$$K = K_{\text{spec}} - K_{\text{photo}} \quad (10)$$

The agreement is very good, suggesting that our method can indeed recover the correct K -corrections based only on broad band magnitudes.

To test how robust these K -correction results are to our model assumptions, we compare them to other methods of calculating fixed frame galaxy magnitudes. An extremely simple method is to calculate the flux in any desired bandpass by fitting a power-law slope and amplitude to the fluxes in the two adjacent bandpasses (extrapolating when necessary). Figure 11 shows the differences in the K -corrections inferred from this method and those inferred from the method of Figure 9, as a function of redshift. r , i , and z are all reasonably similar in either method; u and g , however, have distinct trends with redshift, mostly due to the non-power law nature of the template galaxy spectra (and probably actual galaxy spectra) in this regime. To show this fact, we perform a similar power-law fit, only this time including a break in the spectrum at 4000 Å. We use the $u-g$ color to fit the break, assuming that the slope blueward of 4000 Å is $f(\lambda)/\lambda^2$. Figure 12 shows the results of this fit; the redshift trend in g is greatly reduced, as is the trend in u , but a large amount of scatter remains in the u band. This results from the fact that you can either fit the slope of the SED below the 4000 Å break or the size of the 4000 Å break itself; it is not possible with this data to constrain both in an individual spectrum, which is a limitation of our determination of fixed frame u -band magnitudes.

Finally, it is possible to use the galaxy spectra obtained with the spectrograph to estimate the K -correction for each object. However, this procedure requires trusting the spectrophotometry over a wide

wavelength range. In addition, the region of the galaxy which the spectra cover is not completely well defined. The small scale wavelength features are set by the fiber aperture (θ in diameter) while large scale wavelength features are constrained by a short "smear exposure" which covers a larger area. The smear exposure corrections are clearly the correct approach for point sources, but for galaxies it causes the small scale and large scale features of the spectrum to be determined by somewhat different regions of the galaxy.

Nevertheless, in Figure 13, we compare the K -corrections to $z = 0.1$ of Main Sample galaxies calculated based on the spectra to those of Figure 9, finding that they are extremely similar. There is a trend with redshift in the g -band, which is due to the fact that on average the g color is about 0.1 magnitudes redder in the fiber aperture than in the Petrosian aperture. The implication is that the K -corrections are stronger for the aperture which corresponds to the spectrum than for the Petrosian aperture. This indicates that for work which requires precision, it is best to avoid using the K -corrections determined from the spectra. (Note that in the second paragraph of this section we used the SDSS spectra as example spectra to validate the method; in this paragraph we have evaluated whether to rely on such spectra to calculate K -corrections).

For completeness, Figure 14 compares the spectroscopic and photometric K -corrections to $z = 0.3$ of LRGs. The $^{0.3}r$ and $^{0.3}i$ bands agree very well. However, there is considerable scatter in the $^{0.3}g$ band (nearly equivalent to the $^{0.0}u$ band), at around 20%. Because the LRGs tend to have small color gradients, the issues of fiber sizes and smear exposures are not important in this context.

4. Conclusions and Future Work

We have presented a method and an implementation for estimating galaxy SEDs for the purpose of calculating fixed frame galaxy magnitudes over a range of redshifts. We have demonstrated that it gives sensible and consistent results. We will be using this method in future papers which will describe the joint distribution of luminosities and colors of galaxies, as well as the evolution of the luminosity function of galaxies. Furthermore, we plan to incorporate observations of objects in bands other than the SDSS bands to further describe the nature of galaxy SEDs.

We have not discussed in detail the question of error analysis. There is no answer to this question which is simple, general, and realistic. The photometric errors can of course be propagated to the errors on the reconstructed magnitudes, but these estimates do not describe the errors associated with the restriction to a three-dimensional space of SED shapes. An idea of the level of errors can be gleaned from the comparison of our method to other methods of K -correction. Clearly, r , i and z can be reconstructed to the level of the photometry. Judging from Figure 10, the g band can be reconstructed to about 5% accuracy. The u band is more difficult to evaluate. Judging from the poor reconstructions of the $^{0.3}g$ band (nearly equal to the $^{0.0}u$ band, the reconstructions may be as bad as 20% accuracy.

Topics we have not discussed here are dust- and evolution-correction of the magnitudes. Some of the scatter in the three-dimensional space describing the shape of the galaxy SED is probably due to dust. It may be possible to evaluate the effects of reddening in this space and, by assuming that galaxies corrected for internal reddening live in an even lower dimensional space, perform a reddening correction. We will be investigating this question in the near future. One can perform a similar exercise with evolution estimates, relating the position of a galaxy along the a_1 axis in Figure 3 to a particular star-formation history, and estimating the evolution of the object from that history.

The distribution of galaxies in the three-dimensional space of galaxy SEDs described here may be useful

for other purposes, as well. For example, you can calculate photometric redshifts using the method described here. `kcorrect_v1_10` has a simple (and very fast) photometric redshift estimator with very tight core of residuals (~ 0.05) in a comparison to SDSS galaxies with redshifts. Before this code can be used as a reliable photometric redshift indicator, more work has to be done (which the reader is invited to do using the released code) to identify galaxies which are likely to be redshift outliers. Another use of the three-dimensional space of galaxy SEDs is to create mock samples of galaxies observed in any bandpass at any redshift. We are working on quantifying the correlations between these coefficients and luminosity, surface-brightness and radial profile in order to create mock catalogs which truly reflect the correlations between galaxy properties found in the data.

M B and D W H acknowledge NASA NAG 5-11669 for partial support. M B was supported at the beginning of this work by the DOE and NASA grant NAG 5-7092 at Fermilab. He is also grateful for the hospitality of the Department of Physics and Astronomy at the State University of New York at Stony Brook, who kindly provided computing facilities on his frequent visits there.

Funding for the creation and distribution of the SDSS Archive has been provided by the Alfred P. Sloan Foundation, the Participating Institutions, the National Aeronautics and Space Administration, the National Science Foundation, the U.S. Department of Energy, the Japanese Monbukagakusho, and the Max Planck Society. The SDSS Web site is <http://www.sdss.org/>.

The SDSS is managed by the Astrophysical Research Consortium (ARC) for the Participating Institutions. The Participating Institutions are The University of Chicago, Fermilab, the Institute for Advanced Study, the Japan Participation Group, The Johns Hopkins University, Los Alamos National Laboratory, the Max-Planck-Institute for Astronomy (MPIA), the Max-Planck-Institute for Astrophysics (MPA), New Mexico State University, Princeton University, the United States Naval Observatory, and the University of Washington.

REFERENCES

- Binney, J., & Merrifield, M. 1998, *Galactic Astronomy* (Princeton: Princeton University Press)
- Buzulov, A. G., & Charlot, S. 1993, *ApJ*, 405, 538
- Budavari, T.; Szalay, A. S.; Connolly, A. J.; Csabai, I.; Dickinson, M. (2000), *AJ*, 120, 1588
- Csabai, I., Connolly, A. J., Szalay, A. S., & Budavari, T. 2000, *AJ*, 119, 69
- Eisenstein, D. J., et al. SDSS Collaboration 2001, 122, 2267
- Fan, X. 1999, *AJ*, 117, 2528
- Frei, Z., & Gunn, J. E. 1994, *AJ*, 108, 1476
- Fukugita, M., Ichikawa, T., Gunn, J. E., Doi, M., Shimazaki, K., & Schneider, D. P. 1996, *AJ*, 111, 1748
- Fukugita, M., Shimazaki, K., & Ichikawa, T. 1995, *PASP*, 107, 945
- Gunn, J. E., Carr, M. A., Rockosi, C. M., Sekiguchi, M., et al. 1998, *AJ*, 116, 3040
- Hogg, D. W. 1999, astro-ph/9905116

Oke, J. B., & Gunn, J. E. 1983, *ApJ*, 266, 713

Oke, J. B., & Sandage, A. 1968, *ApJ*, 154, 21

Petrosian, V. 1976, *ApJ*, 209, L1

Press, W. H., Teukolsky, S. A., Vetterling, W. T., & Flannery, B. P. 1992, *Numerical Recipes* (Cambridge: Cambridge Univ. Press)

Schlegel, D. J., Finkbeiner, D. P., & Davis, M. 1998, *ApJ*, 500, 525

Schlegel, D. J., et al. 2002, in preparation

Smith, J. A., et al. SDSS Collaboration 2002, *AJ*, 123, 2121

Stoughton, C., et al. 2002, *AJ*, 123, 485

Strauss, M. A., et al. 2002, submitted to *AJ*

Subbarao, M., et al. 2002, in preparation

York, D., et al. 2000, *AJ*, 120, 1579

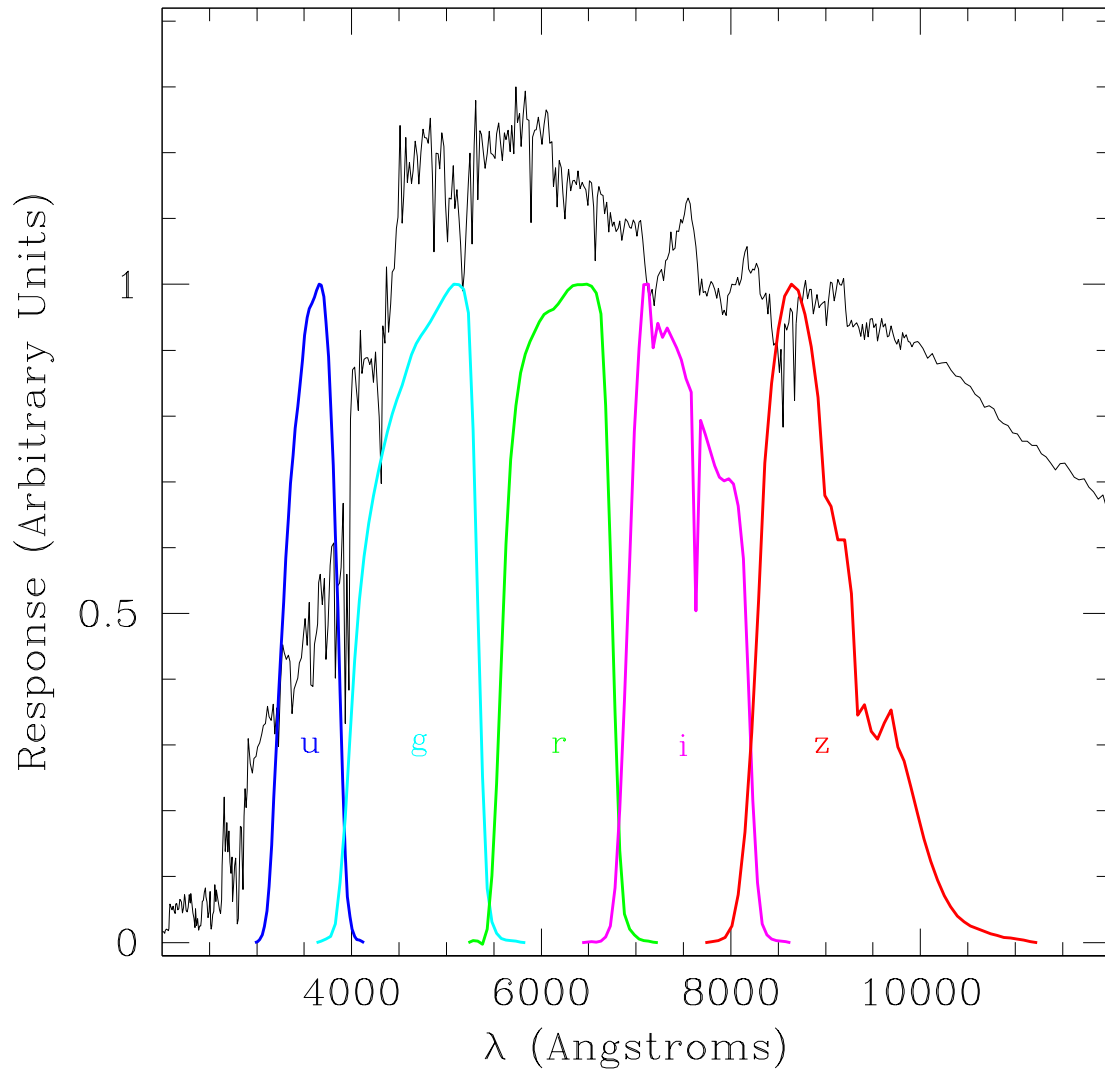


Fig. 1. Estimated filter response for all five bands in the SDSS, as a function of observed wavelength, as measured by Mamoru Doi. A 4 Gyr old instantaneous burst using the models of Bruzual & Charlot (1993) (and observed at $z = 0$) is shown for reference.

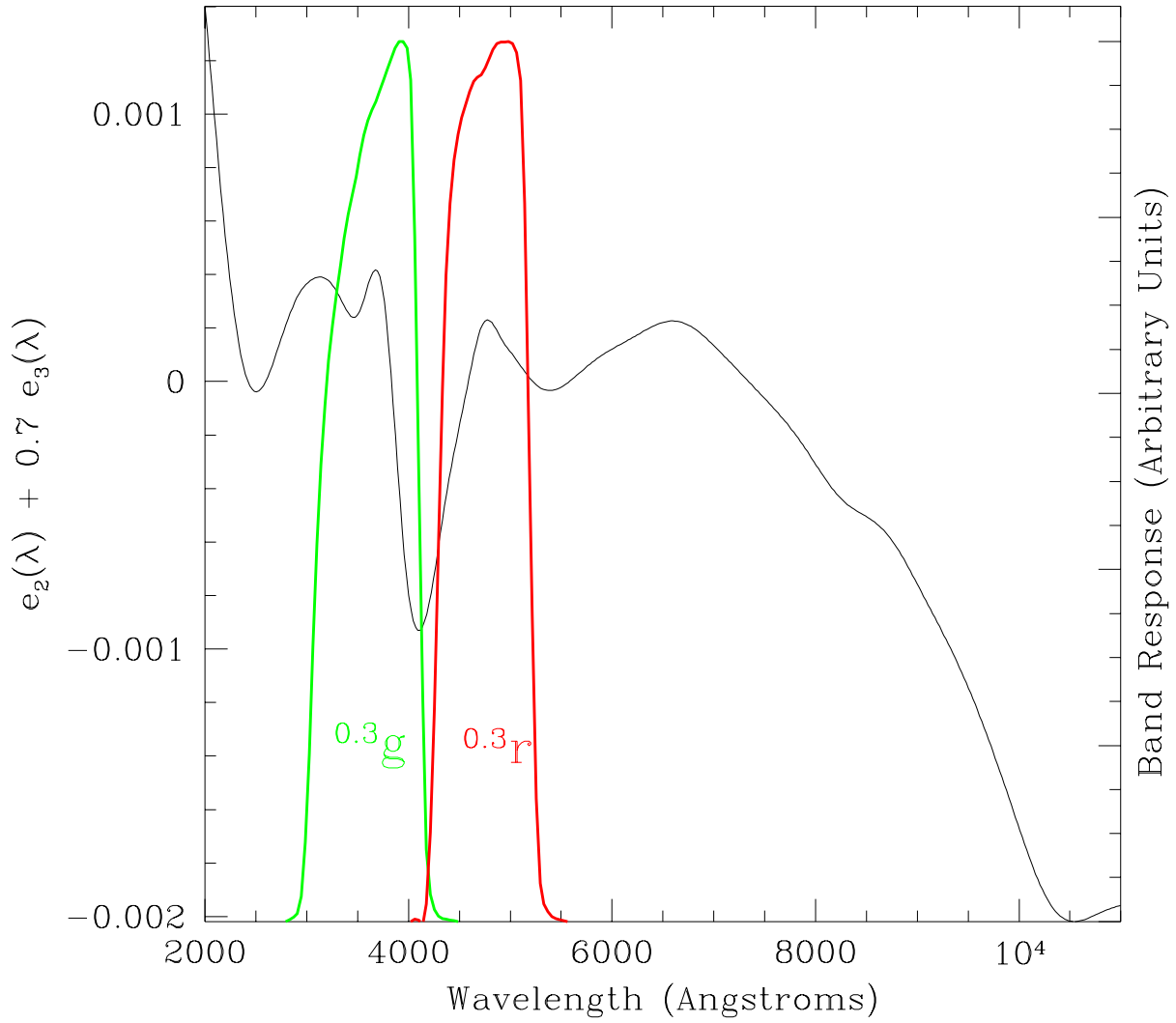


Fig. 2. The spectrum corresponding to the direction of the spur in the upper right panel of Figure 3. Note the strong feature near 4000 Å. Overplotted are the bandpasses for $z=0.3$ g and $z=0.3$ r . The strong features fall in the gap between the bandpasses. Thus, in a linear fit to a galaxy at $z=0.3$, this component can be used to fit the observed magnitudes without being constrained to have reasonable behavior around 4000 Å.

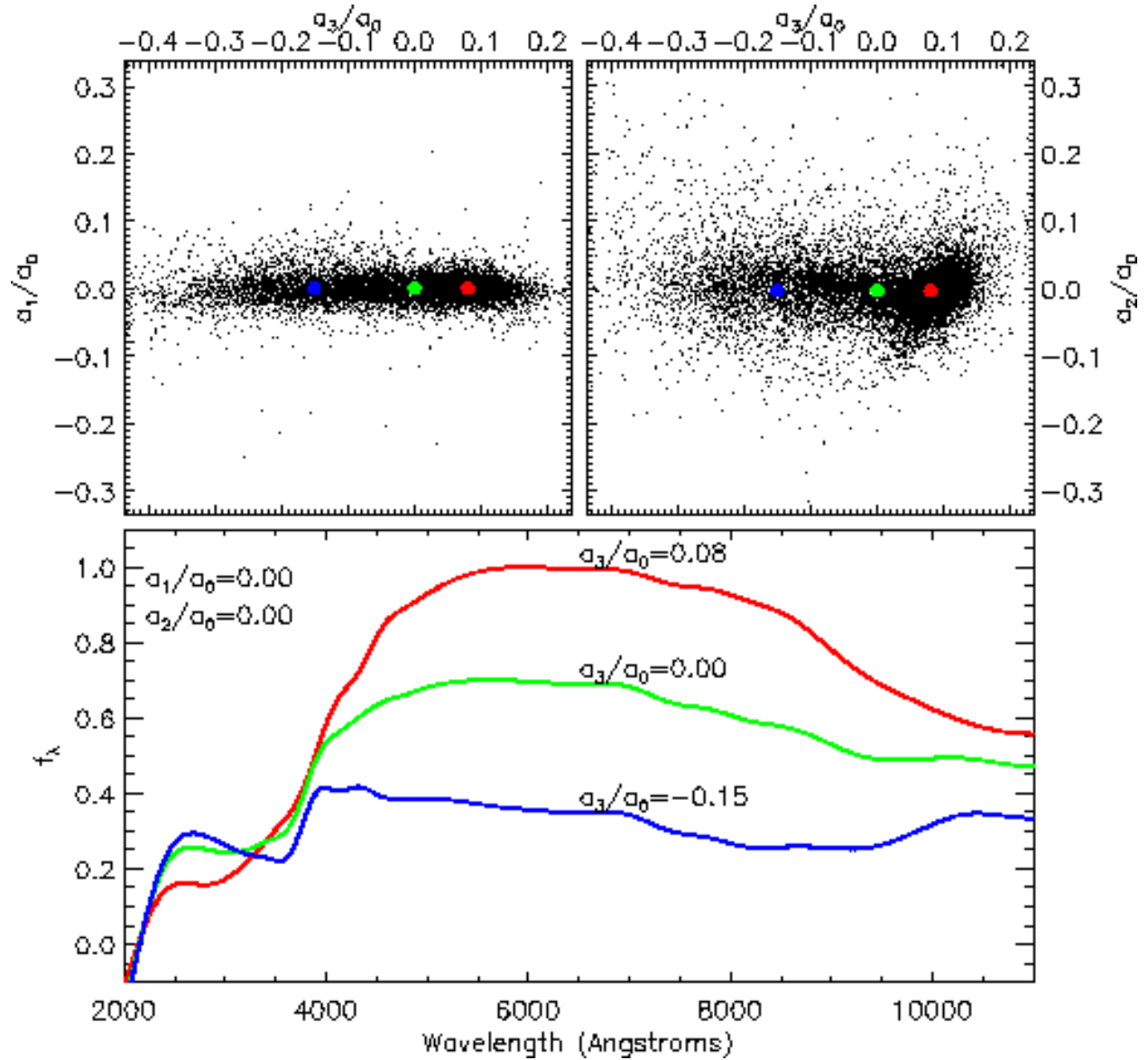


Fig. 3. Top panels: Distribution of the components of the four-parameter fit to the r-band SDSS photometry for a random subsample consisting of 10,000 of the SDSS galaxies. a_0 is linearly proportional to the flux between 3500 Å and 7500 Å, while a_1 , a_2 , and a_3 contribute no flux in this range. Thus, the ratios a_1/a_0 , a_2/a_0 , and a_3/a_0 describe the spectral type of the galaxy. a_1/a_0 is the most variable parameter and thus is the best separator of galaxy type. The spur extending from the upper left to the lower right from the red dot in the $(a_3/a_0)-(a_1/a_0)$ plane is due to a degeneracy for galaxies at $z \approx 0.3$, described in detail in Section 3.3. Bottom panel: At fixed a_2/a_0 and a_3/a_0 , the inferred spectra corresponding to various values of a_3/a_0 . Near $a_3/a_0 = 0.20$, the spectrum is similar to that of an elliptical galaxy. For higher values, the spectrum becomes bluer.

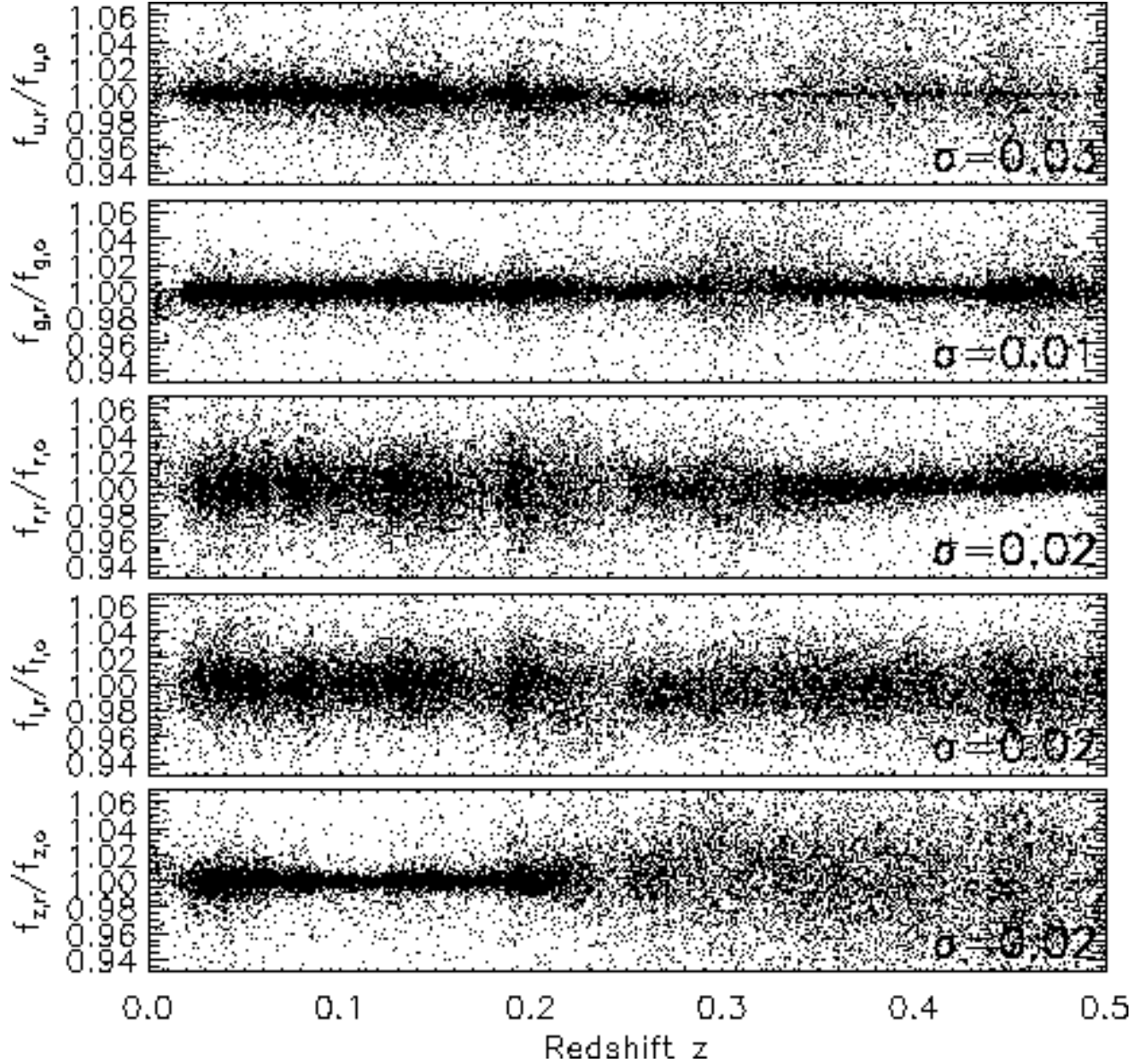


Fig. 4. | Reconstructed galaxy fluxes relative to the observed galaxy fluxes, for all five SDSS bands, shown for a random subsample consisting of around 10,000 of the SDSS galaxies. The residuals are shown against redshift. There is no systematic trend with redshift in any band. The 5-sigma clipped estimate of the scatter around the observed fluxes is listed for each band. In u, g, r, and i the scatter is consistent with the expected photometric errors in the survey at all redshifts. At high redshift the scatter in z becomes large, most likely due to increasing photometric errors.

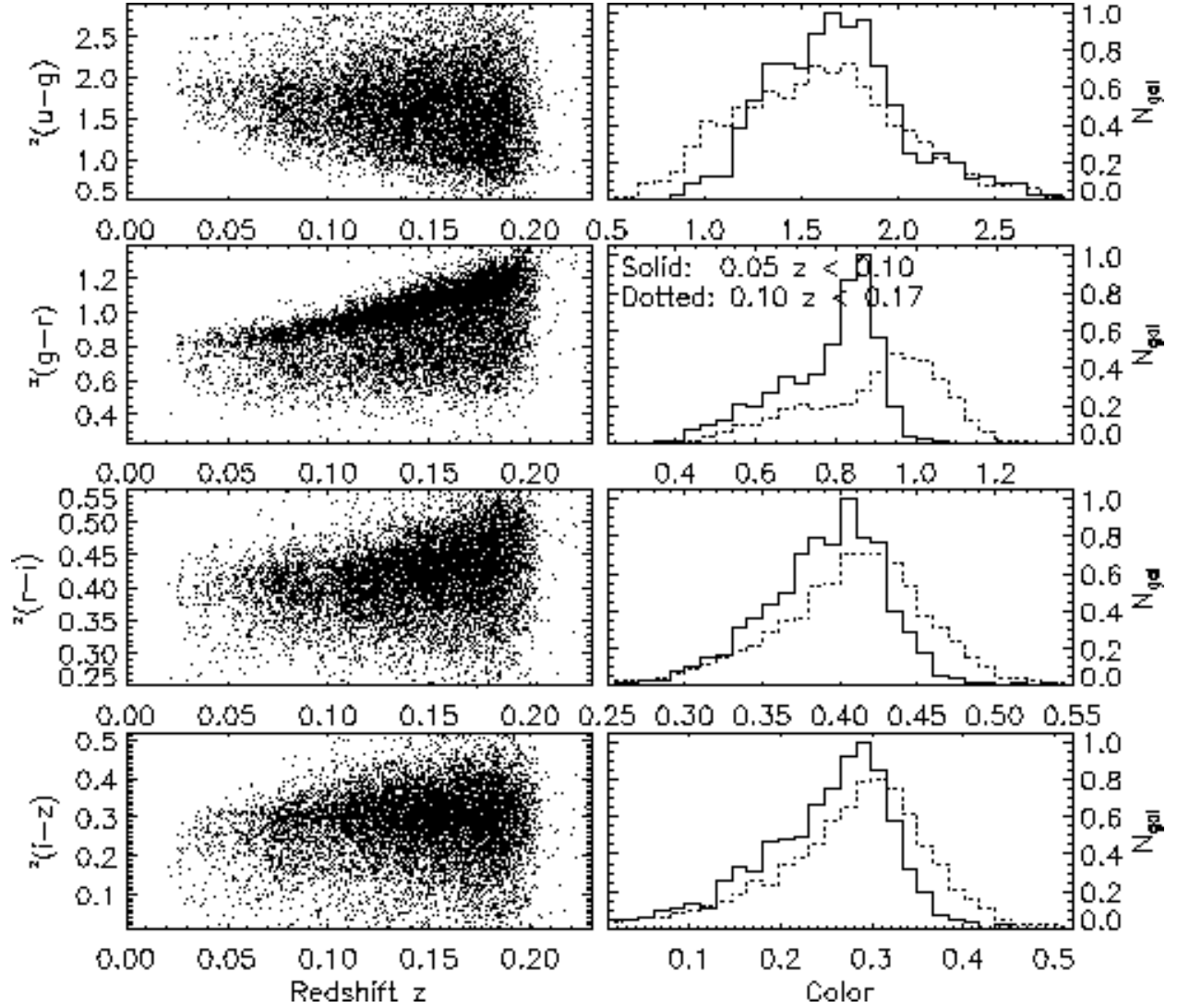


Fig. 5. Color distributions in the observed frame for SDSS Main Sample galaxies in the luminosity range $-21.5 < M_{0.1\mu} < -21.2$. This sample is complete (that is, volume limited) for $0.05 < z < 0.17$. Left panels show the colors as a function of redshift. Right panels show the distributions of each color at high and low redshift within the volume-limited subsample. The observed colors clearly depend strongly on redshift.

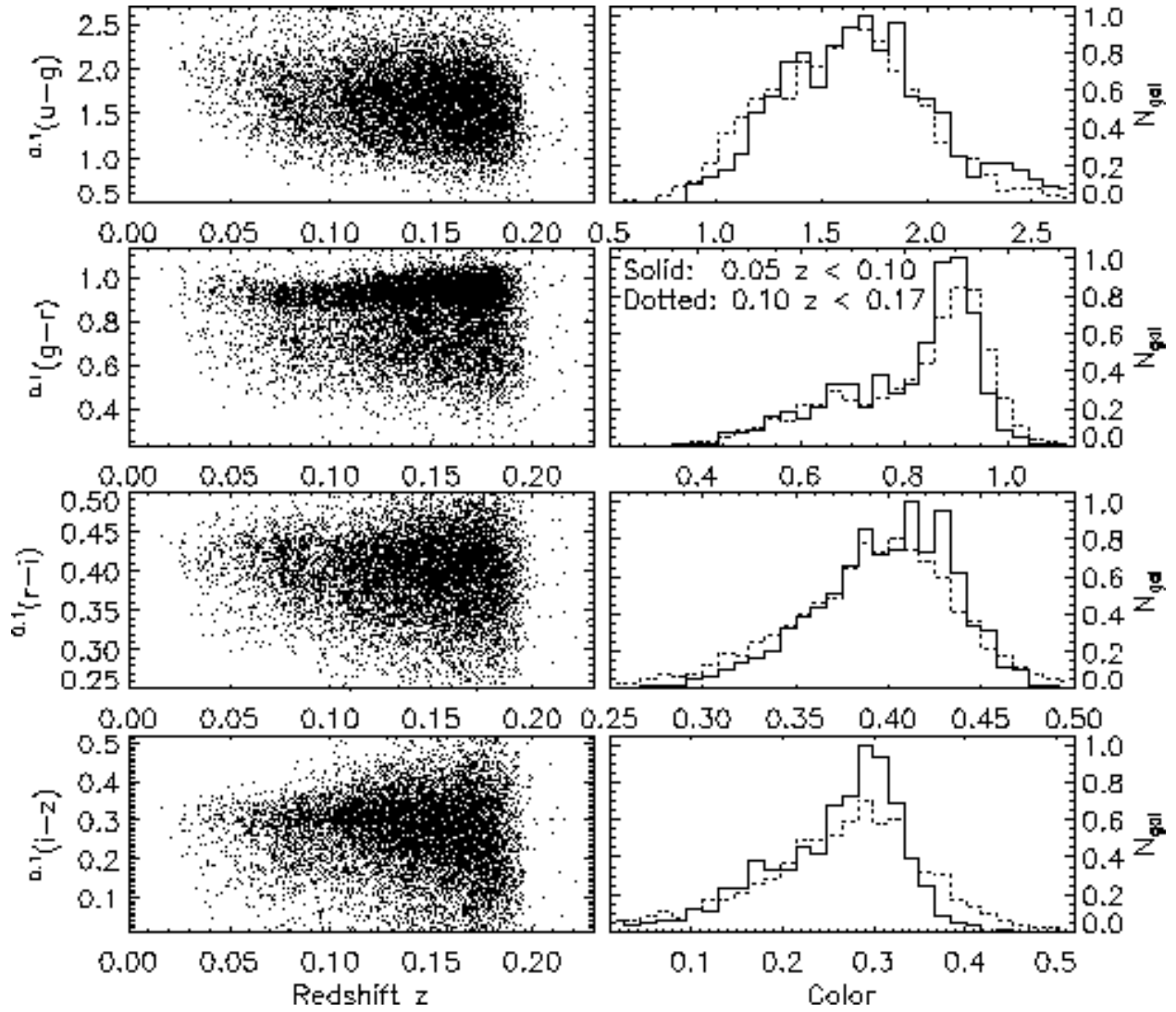


Fig. 6. | Similar to Figure 5, but now the colors are K-corrected to $z = 0.1$. There is very little dependence of the colors on redshift, even for the $^{0.1}u$ band, where the low-redshift end is an extrapolation of the data.

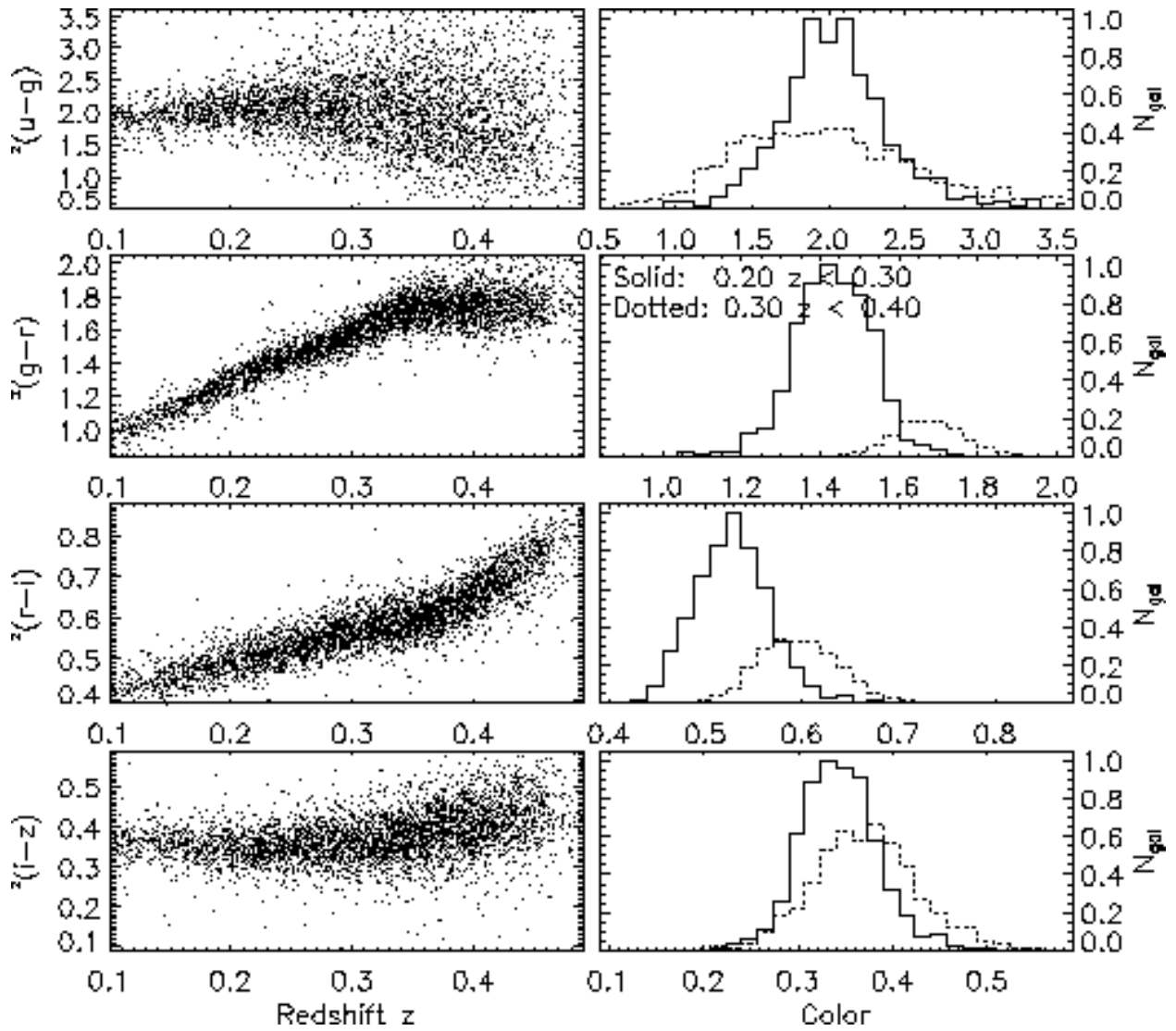


Fig. 7. | Similar to Figure 5, now showing LRG galaxies (Cut I) in the luminosity range $-22.8 < M_{0.3r} < -22.5$. A gain, there is a strong dependence on redshift.

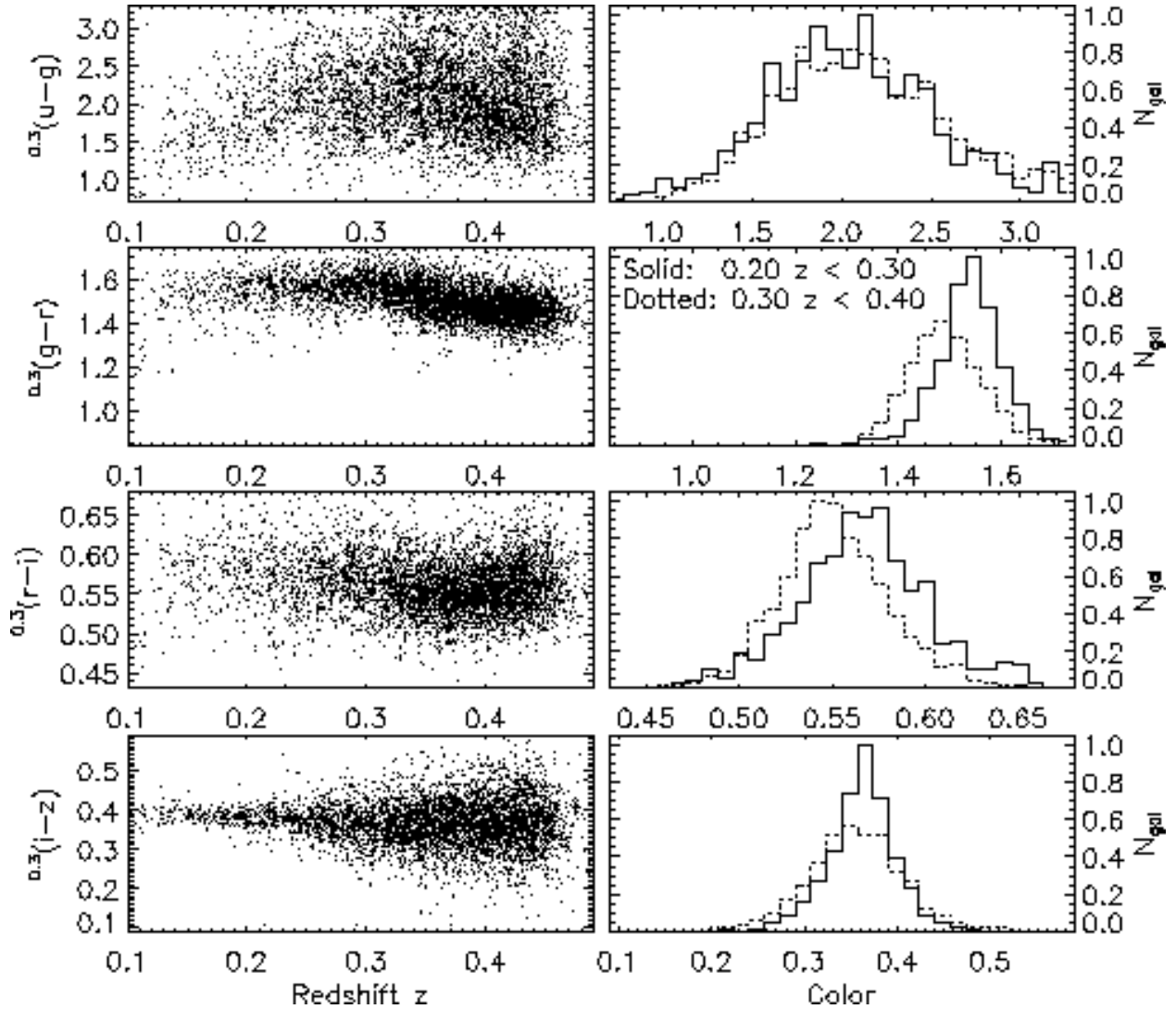


Fig. 8. | Same as Figure 7, now K-correcting the LRG galaxies to $z = 0.3$. The redshift dependence is greatly reduced for the LRGs in comparison to Figure 7; on the other hand, there are distinct trends of restframe color with redshift. In $^{0.3}(g-r)$ an overall trend is apparent; LRGs at $z = 0.4$ are about 0.1 magnitudes bluer than LRGs at $z = 0.2$. A change of this magnitude is attributable to passive galaxy evolution, though considerably more work needs to be done to show that this is occurring. In $^{0.3}(r-i)$, a blueward shift also occurs, though at a much smaller level.

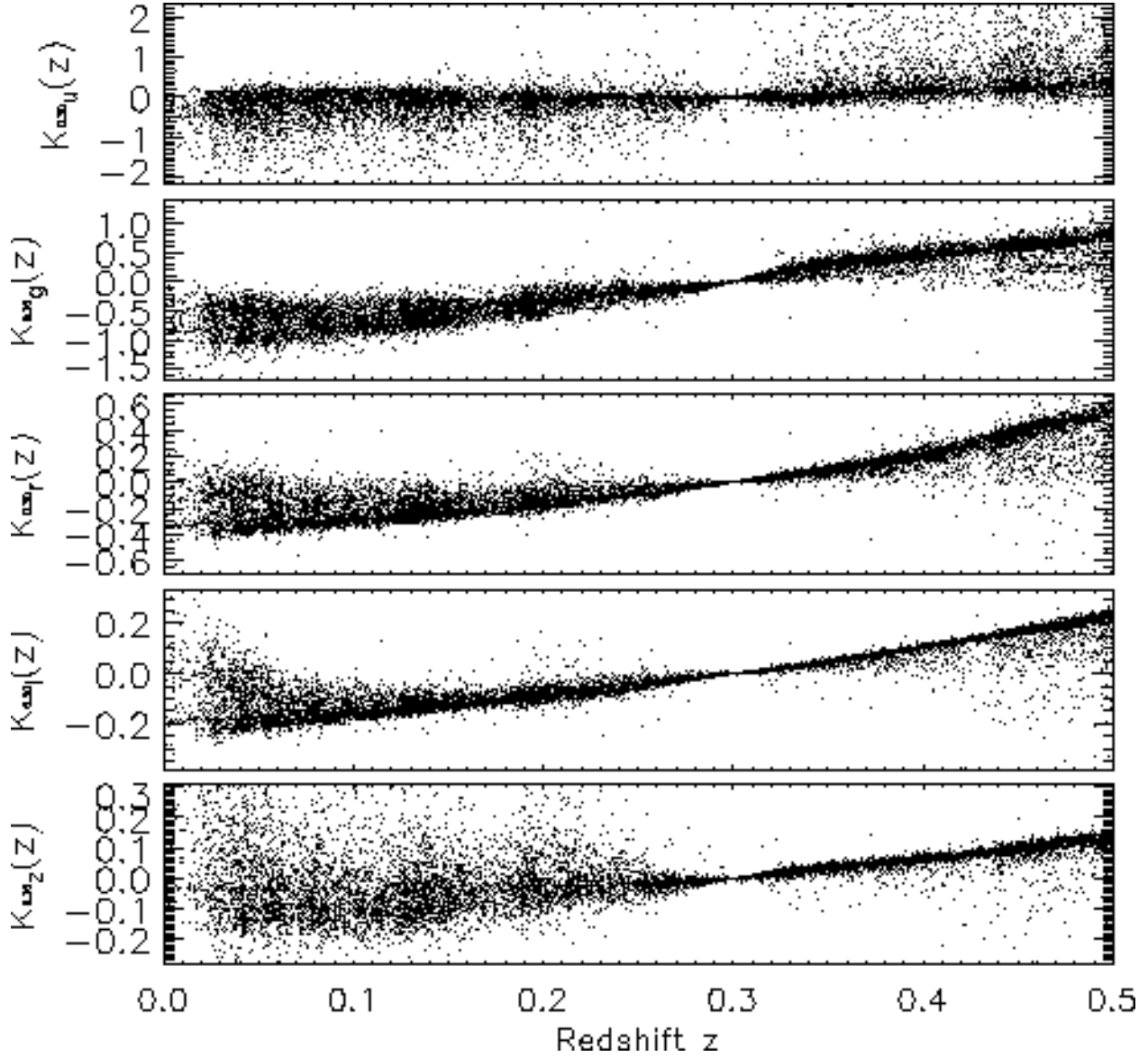


Fig. 9. | K -corrections to $z = 0.3$ as a function of redshift in all ve bands for a random subsam ple consisting around 10,000 of the SD SS galaxies. The range of K -corrections at each redshift re flects the range of galaxy types at each redshift. The K -corrections are largest, and therefore the most uncertain, for the $^{0.3}u$ and $^{0.3}g$ bands. While we show the K -corrections for $^{0.3}u$ at $z < 0.3$ and for $^{0.3}z$ at $z > 0.3$, and indeed these K -corrections are fairly well-behaved, we do not recom mend using these extrapolated results for scienti c purposes.

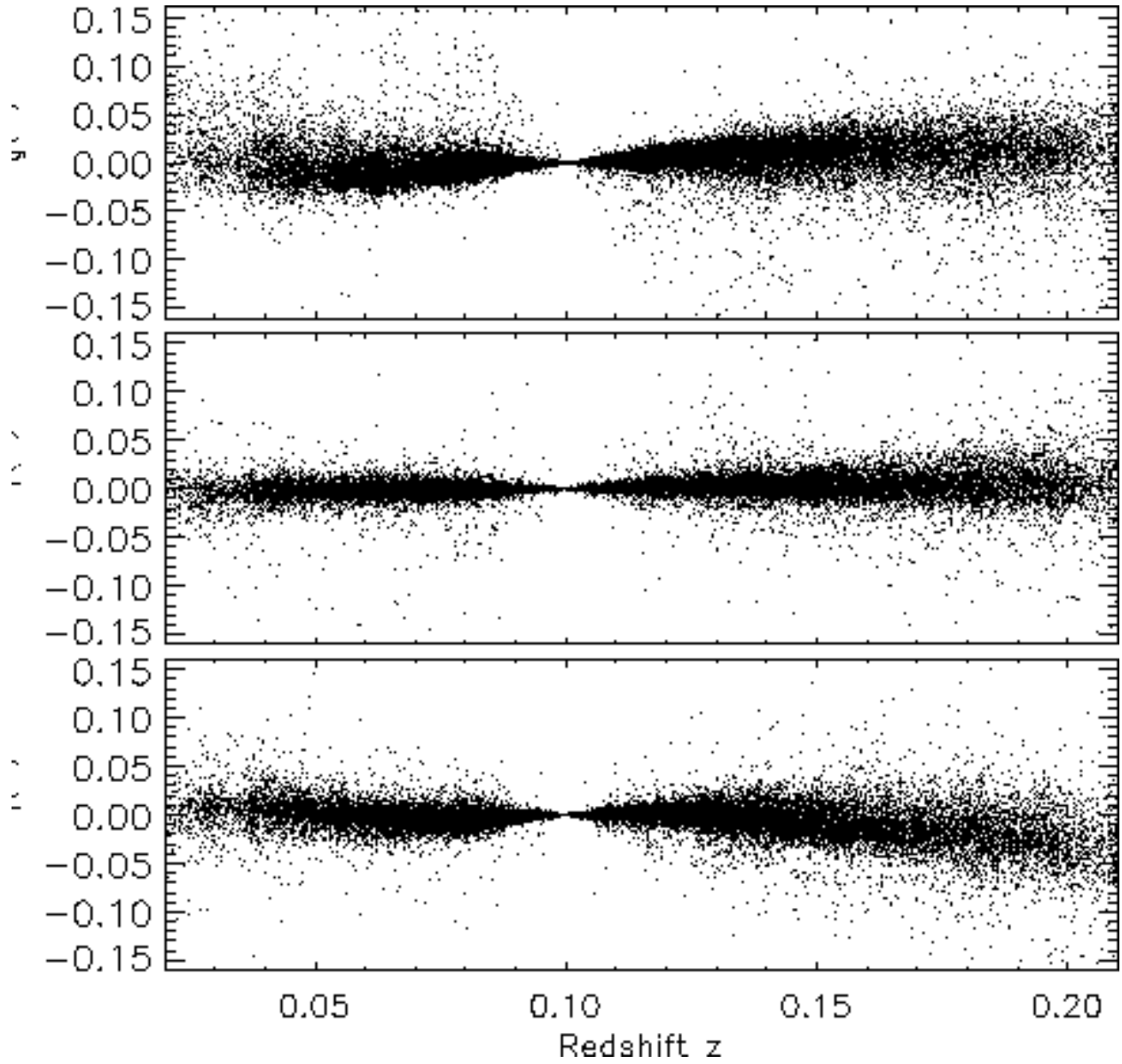


Fig. 10. | Difference between the K-corrections to $z = 0.1$ determined from the spectroscopy and those determined from the analysis of broad-band magnitudes synthesized from the same spectra.

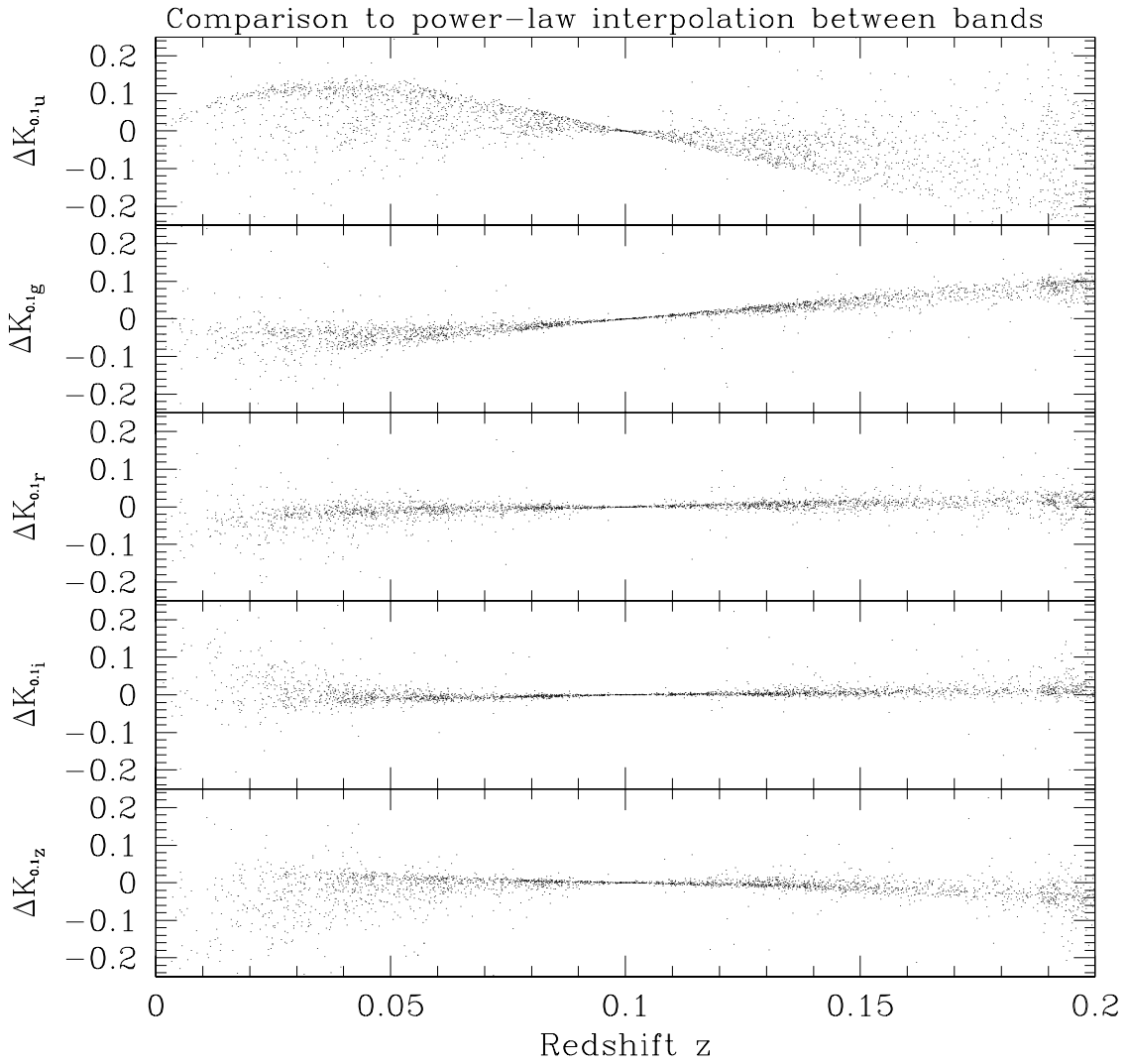


Fig. 11. | Difference in the K-corrections to $z = 0.1$ in each band between the method used in Figure 9 and the method of simply interpolating between adjacent bands fitting a power-law SED. The differences are small in $^{0.1}r$, $^{0.1}i$, and $^{0.1}z$, where galaxy SEDs have simple shapes. There are large systematic differences in $^{0.1}u$ and $^{0.1}g$, for which the 4000 Å break is important in the spectral templates used.

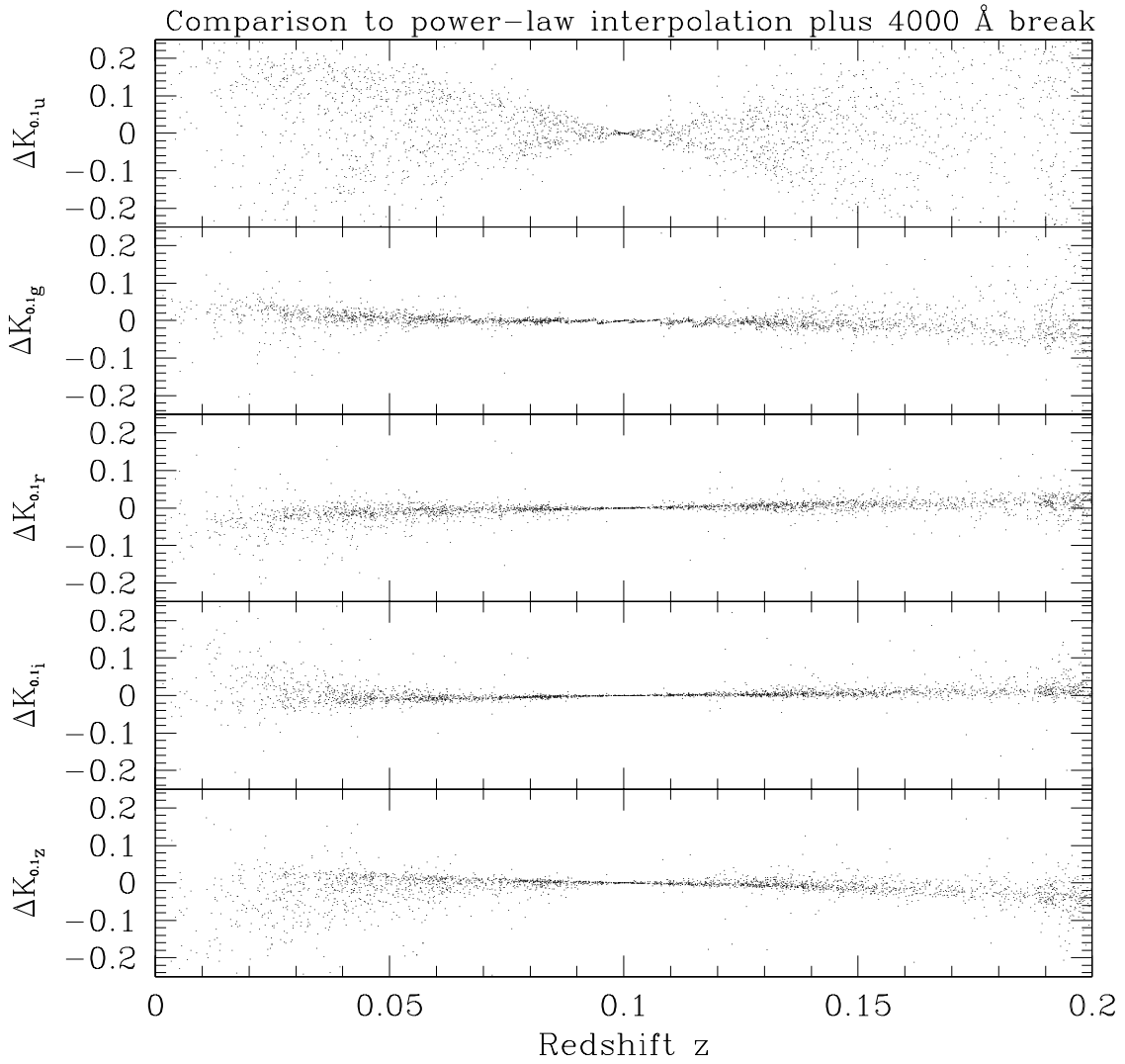


Fig. 12. | Same as Figure 11, now comparing to a method of interpolating the bandpasses using power-laws, and fitting for the 4000Å break. The systematic trends in $^{0.1}u$ and $^{0.1}g$ are gone (though there is considerable scatter in $^{0.1}u$).

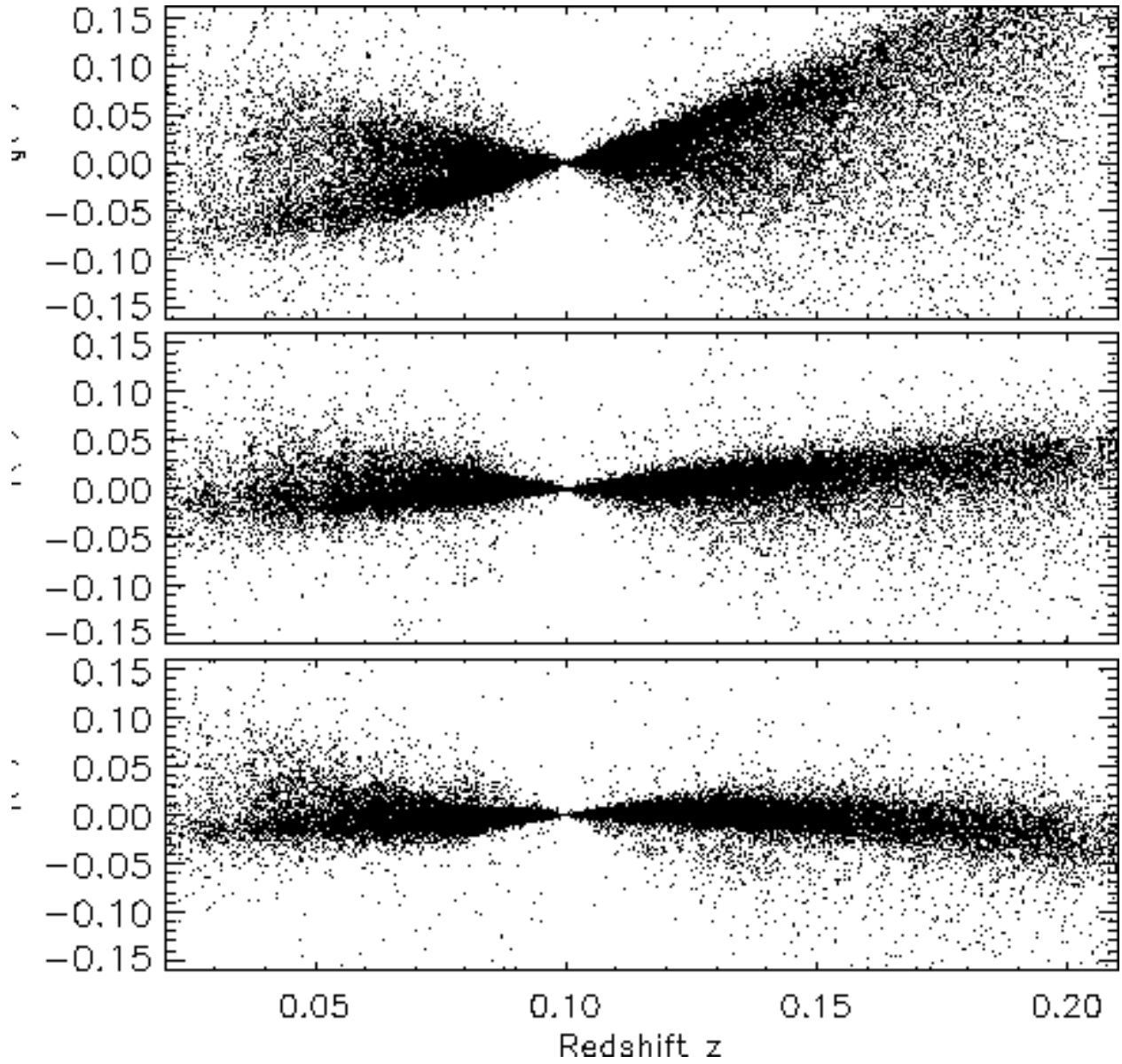


Fig. 13. | Difference between the K-corrections to $z = 0.1$ determined from the spectroscopy and those determined from the analysis of the broad-band Petrosian magnitudes, for Main Sample galaxies.

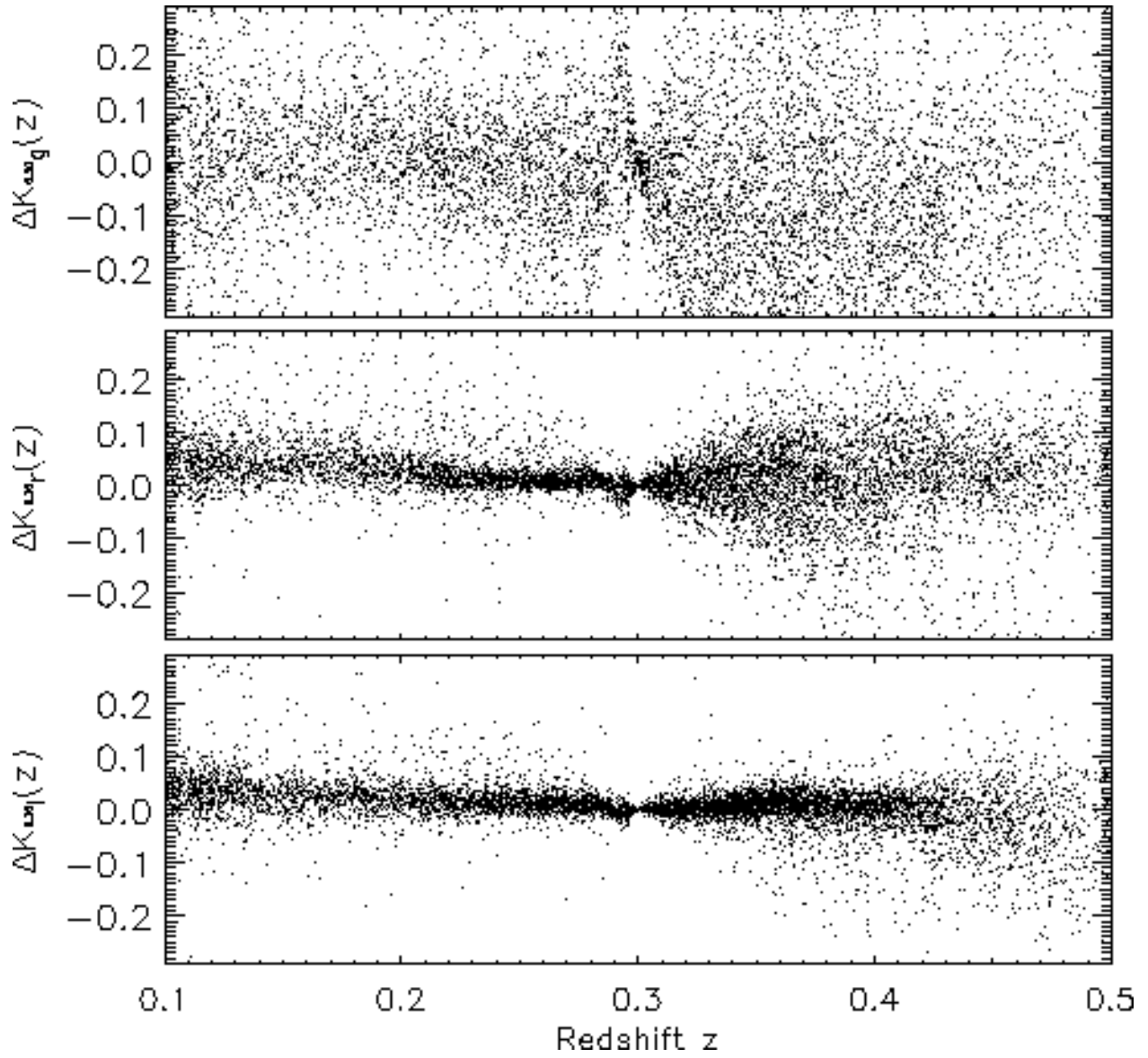


Fig. 14. | Difference between the K-corrections to $z = 0.3$ determined from the spectroscopy and those determined from the analysis of the broad-band model magnitudes, for LRGs.